

Diurnal modulation due to self-interacting mirror & hidden sector dark matter

R. Foot¹

*ARC Centre of Excellence for Particle Physics at the Terascale,
School of Physics, University of Melbourne,
Victoria 3010 Australia*

Mirror and more generic hidden sector dark matter models can simultaneously explain the DAMA, CoGeNT and CRESST-II dark matter signals consistently with the null results of the other experiments. This type of dark matter can be captured by the Earth and shield detectors because it is self-interacting. This effect will lead to a diurnal modulation in dark matter detectors. We estimate the size of this effect for dark matter detectors in various locations. For a detector located in the northern hemisphere, this effect is expected to peak in April and can be detected for optimistic parameter choices. The diurnal variation is expected to be much larger for detectors located in the southern hemisphere. In particular, if the CoGeNT detector were moved to e.g. Sierra Grande, Argentina then a 5σ dark matter discovery would be possible in around 30 days of operation.

¹E-mail address: rfoot@unimelb.edu.au

1 Introduction

Mirror[1] and more generic hidden sector dark matter models provide a consistent explanation[2, 3, 4] of the DAMA annual modulation signal[5], as well as the low energy energy excess seen in the CoGeNT[6] and CRESST-II[7] experiments. This explanation is consistent with the constraints from higher threshold experiments, such as CDMS[8] and XENON100[9] when reasonable systematic uncertainties in energy scale are considered².

A distinctive feature of mirror and more generic hidden sector dark matter models is that the dark matter particles are self-interacting. This means that dark matter captured by the Earth can effectively block the halo dark matter wind. This effect will also lead to a diurnal modulation of detector dark matter signals. The purpose of this paper is to study this effect. Although we focus particular attention on mirror and more generic hidden sector dark matter models with unbroken $U(1)'$ interaction, our study would be of relevance to many other self-interacting dark matter models[13].

Diurnal modulation of a dark matter signal can also occur due to elastic scattering of dark matter on the constituent nuclei of the Earth[14]. In that case, the effect is typically small unless the dark matter abundance is much less than expected. We will show that the diurnal effect arising from the self-interactions of mirror/hidden sector particles can be much larger. In particular, for a detector located in the southern hemisphere, the diurnal modulation effect is anticipated to be maximal, with a rate suppression varying between zero and near 100% for a detector located in e.g. Sierra Grande, Argentina. In fact, a dark matter experiment was conducted there in the 1990's[15]. Unfortunately, the energy threshold was too high to detect a significant rate of dark matter interactions in that experiment. However, CoGeNT's low threshold detector is highly portable and could easily be moved from the Soudan laboratory to e.g. Sierra Grande. This would allow the diurnal modulation to be detected with 5σ C.L. in around 30 days of operation.

2 Mirror & hidden sector dark matter

Mirror[1] and the more generic hidden sector dark matter models[2, 16] assume the existence of a hidden sector which contains an unbroken $U(1)'$ gauge interaction which is mixed with the standard $U(1)_Y$ via renormalizable kinetic mixing

²There are also lower threshold analysis by the XENON10[10] and CDMS collaborations[11]. However it has been argued[12] that neither analysis can exclude light dark matter when systematic uncertainties are properly taken into account.

interaction:[17, 1]

$$\mathcal{L}_{mix} = \frac{\epsilon'}{2 \cos \theta_w} F^{\mu\nu} F'_{\mu\nu} \quad (1)$$

where $F_{\mu\nu}$ is the standard $U(1)_Y$ gauge boson field strength tensor, and $F'_{\mu\nu}$ is the field strength tensor for the hidden sector $U(1)'$. This interaction enables hidden sector $U(1)'$ charged particles (of charge Qe) to couple to ordinary photons with electric charge $Q\epsilon'e \equiv \epsilon\epsilon'$ [18]. [In the case of mirror dark matter, $\epsilon' = \epsilon/\cos\theta_w$]. We consider the case where the hidden sector contains two (or more) stable $U(1)'$ charged dark matter particles, F_1 and F_2 with masses m_1 and m_2 . Under the standard assumptions of a dark halo forming an isothermal sphere, the condition of hydrostatic equilibrium relates the halo temperature of the particles to the galactic rotational velocity, $v_{rot} \sim 240$ km/s:

$$T = \frac{1}{2} \bar{m} v_{rot}^2 \quad (2)$$

where $\bar{m} \equiv \frac{n_{F_1} m_1 + n_{F_2} m_2}{n_{F_1} + n_{F_2}}$ is the mean mass of the particles in the galactic halo. We have assumed that the self interactions mediated by the unbroken $U(1)'$ gauge interactions are sufficiently strong so that they thermalize the hidden sector particles, F_1 and F_2 . The interaction length is typically much less than a parsec[19] and the dark matter particles form a pressure-supported halo. The dark matter particles are then described by a Maxwellian distribution with $f_i(v) = \exp(-E/T) = \exp(-\frac{1}{2}m_i v^2/T) = \exp[-v^2/v_0^2(i)]$ where

$$v_0(i) = v_{rot} \sqrt{\frac{\bar{m}}{m_i}}. \quad (3)$$

With the assumptions that $m_2 \gg m_1$ and that the abundance of F_2 is much less than F_1 , we have that $v_0^2(F_2) \ll v_{rot}^2$. The narrow velocity dispersion (recall $\sigma_v^2 = 3v_0^2/2$) can greatly reduce the rate of dark matter interactions in higher threshold experiments such as CDMS[8] and XENON100[9] whilst still explaining the signals in the lower threshold DAMA and CoGeNT experiments.

Mirror dark matter refers to the specific case where the hidden sector is an exact copy of the standard model sector[1] (for a review and more complete list of references see ref.[20])³. In that case a spectrum of dark matter particles of known masses are predicted: e' , H' , He' , O' , Fe' ,... (with $m_{e'} = m_e, m_{H'} = m_H$, etc). The galactic halo is then presumed to be composed predominately of a spherically

³Note that successful big bang nucleosynthesis and successful large scale structure requires effectively asymmetric initial conditions in the early Universe, $T' \ll T$ and $n_{b'}/n_b \approx 5$. See ref.[21] for further discussions.

distributed self interacting mirror particle plasma comprising these particles[22]. Ordinary and mirror particles interact with each other via kinetic mixing of the $U(1)_Y$ and its mirror counterpart.

Both mirror and the more generic hidden sector dark matter models can explain the direct detection experiments[2, 3, 4, 23, 24]. These scenarios involve kinetic mixing induced elastic (Rutherford) scattering of the dark matter particles off target nuclei. In the mirror dark matter case, the DAMA/CoGeNT signals are assumed to arise from the scattering of the dominant mirror metal component, A' , off target nuclei. [The He' and H' components are too light to give a signal above the DAMA/CoGeNT energy threshold]. In the case of generic hidden sector models the role of A' is played by F_2 . Such elastic scattering can explain the normalization and energy dependence of the DAMA annual modulation amplitude and also the CoGeNT and CRESST-II spectrum consistently with the null results of the other experiments, and yields a measurement of $\epsilon\sqrt{\xi_{A'}}$ and $m_{A'}/m_{F_2}$. In the case of mirror dark matter the favoured parameter space is[4, 3]:

$$\begin{aligned}\epsilon\sqrt{\xi_{A'}} &\approx \text{few} \times 10^{-10}, \\ \frac{m_{A'}}{m_p} &\approx 16 - 56\end{aligned}\tag{4}$$

where $\xi_{A'} \equiv n_{A'}m_{A'}/(0.3 \text{ GeV}/\text{cm}^3)$ is the halo mass fraction of the species A' and m_p is the proton mass. In the case of the generic hidden sector model, ϵ is about an order of magnitude larger. [The difference arises because in our notation the kinetic mixing induces an electric charge $\epsilon Z'e$ for mirror dark matter and ϵe for the generic hidden sector case].

As briefly discussed in Eq.(3) above, the velocity dispersion of the halo A'/F_2 particles depends on the parameter \bar{m} . In the mirror model with isothermal halo it can be estimated[25] to be around 1.1 GeV although it might vary somewhat from this value. For example, if the e' have a lower temperature than the mirror nuclei in the halo then \bar{m} can be somewhat larger, with an upper limit of around 3 GeV. Although realistically it is unlikely that \bar{m} could be this large in the mirror model, we consider this value in our numerical work as an extremely optimistic case which might also be relevant to more generic hidden sector models where the parameter \bar{m} is less constrained.

3 Distribution of mirror dark matter captured by the Earth and its shielding radius - R_0

In the following sections we restrict our attention to the case of mirror dark matter for definiteness. The more generic hidden sector scenario is completely analogous.

Mirror particles will occasionally be captured by the Earth and accumulate in the Earth's core. Once a significant population of mirror particles have been accumulated, mirror dark matter will be captured at a rate:

$$\frac{dN}{dt} \sim \pi R_0^2 f_{A'} \quad (5)$$

where $f_{A'} \approx v_{rot} \xi'_{A'} \frac{0.3 \text{ GeV/cm}^3}{m_{A'}}$ is the flux of A' mirror particles hitting the Earth. Here R_0 is the maximum distance from the Earth's center for which dark matter can be captured due to self interactions. We will show in a moment that this distance is (currently) of order 4,000 km for the example where $m_{A'} \approx 22m_p$. Thus we anticipate that around

$$\begin{aligned} N &\sim \int \pi R_0^2 f_{A'} dt \\ &\sim 10^{39} \left(\frac{\xi_{A'}}{10^{-1}} \right) \end{aligned} \quad (6)$$

A' particles will be captured during the five billion year history of the Earth. This is many orders of magnitude within the geophysical limits[26].

A mirror particle, once trapped in the Earth, will lose energy rapidly due to interactions with the ordinary matter. The Rutherford cross section increases rapidly as the relative velocity decreases, $d\sigma/d\Omega \propto 1/v^4$, and thus one expects the captured mirror particles to rapidly thermalize with the ordinary matter. Their distribution can then be obtained from the condition of hydrostatic equilibrium:

$$\begin{aligned} \frac{dP}{dr} &= -\rho_{A'} g \\ \frac{dn_{A'}}{dr} &= -\frac{n_{A'}}{T} \left[m_{A'} g + \frac{dT}{dr} \right] \end{aligned} \quad (7)$$

where we have used $P = n_{A'} T$ and $\rho_{A'} = m_{A'} n_{A'}$. Note that we have implicitly assumed that captured mirror nuclei and mirror electrons combine into mirror atoms. The gravitational acceleration, g , is given in terms of the mass density ρ ,

$$g = \frac{G}{r^2} \int_0^r \rho 4\pi r'^2 dr' . \quad (8)$$

Note that both g and T depend on r . We model the Earth's density and temperature as given in figures 1a, 1b. The boundaries in figure 1a correspond to the inner core, core, and mantle. In each of these regions we use a linear approximation for the density adapted from the Preliminary Reference Earth Model[27].

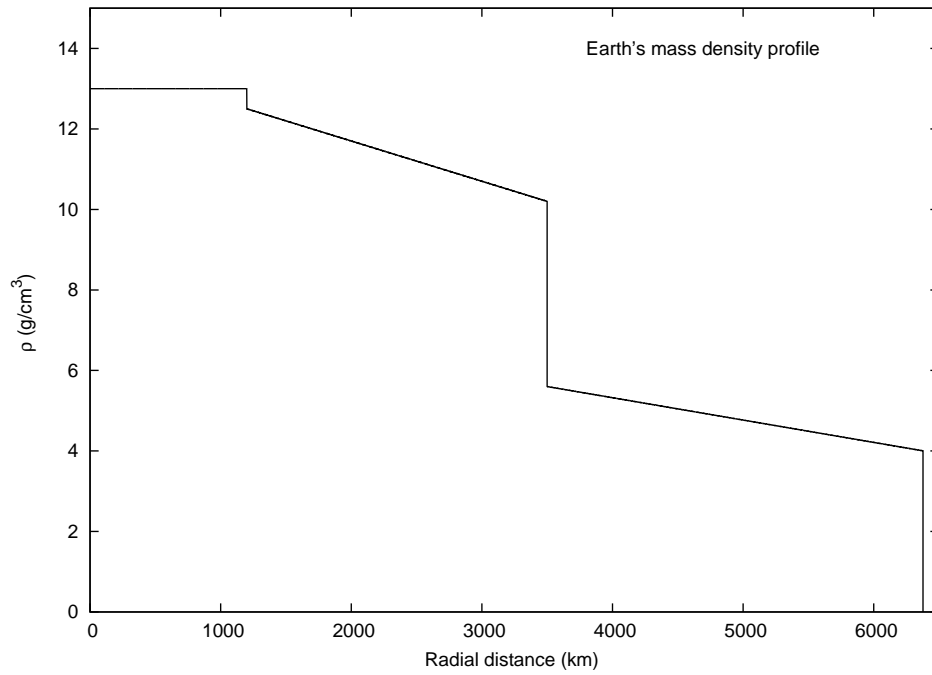


Figure 1a: Earth's mass density [g/cm³] versus radial distance.

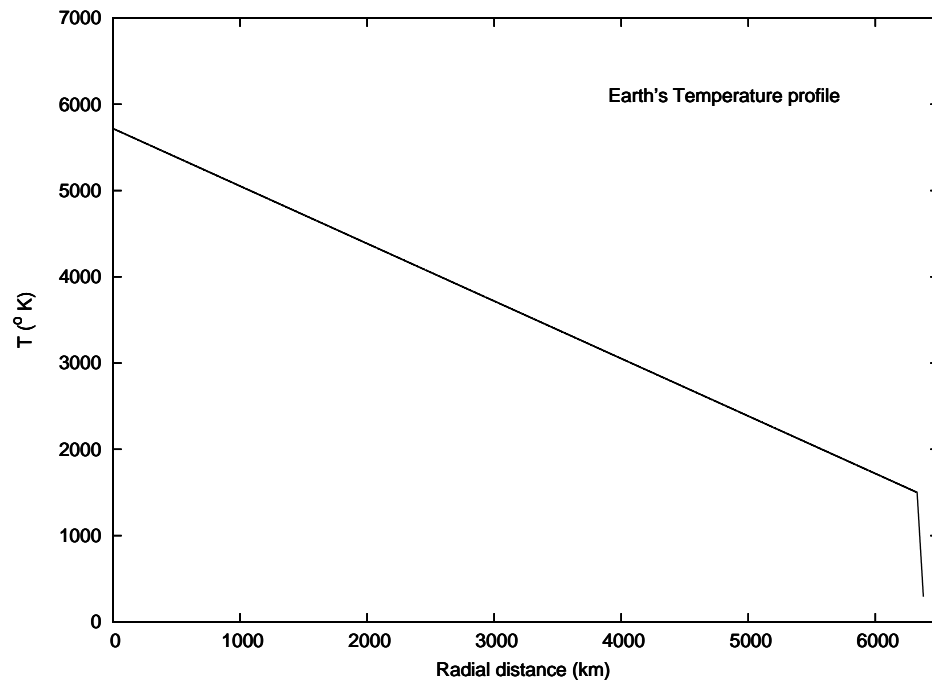


Figure 1b: Earth's temperature profile [°K] versus radial distance.

Eq.(7) can be numerically solved for $n_{A'}(r)$, taking into account the dependence of g and T on r . The result is shown in figure 2. If the total number of accumulated A' particles is around 10^{39} , as indicated in Eq.(6), then we find that the central number density is of order $n_{A'}(0) \sim 10^{14} \text{ cm}^{-3}$.

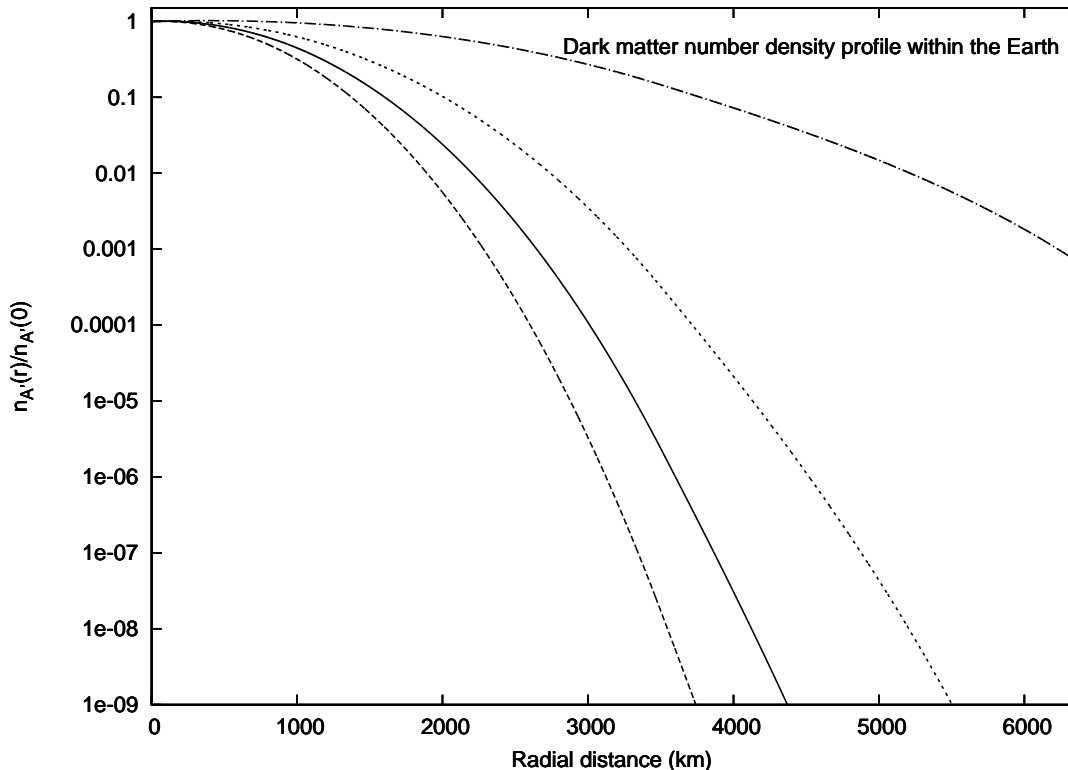


Figure 2: The distribution within the Earth, $n_{A'}(r)/n_{A'}(0)$, of captured mirror particles of mass $m_{A'} = 22m_p$ (solid line), $m_{A'} = 30m_p$ (dashed line), $m_{A'} = 14m_p$ (dotted line) and $m_{A'} = 4m_p$ (dashed-dotted line).

Figure 2 suggests that any captured He' particles will quickly escape the Earth. Indeed, the He' distribution is quite spread out, and particles in the tail of their Maxwellian velocity distribution can have velocities much greater than the Earth's escape velocity. One can easily show[23] that e.g. He' particles with velocities $\gtrsim 20$ km/s can travel $\gtrsim 100$ km through ordinary matter without significant energy loss and escape the Earth's gravity (assuming here $\epsilon \lesssim 10^{-9}$). Heavier mirror particles on the other hand are much more tightly confined within the Earth and have negligible probability of escaping Earth's gravity.

The captured mirror dark matter in the Earth can potentially shield a detector from halo dark matter particles if they originate from a direction which takes them through the Earth. Whether or not a halo dark matter particle will get shielded will depend on how close its trajectory takes it to the center of the Earth, where the density of Earth bound dark matter particles is greatest. Let us define r_0 as the distance of closest approach to the Earth's center of a given particle trajectory. Let us now work out the maximum value of r_0 , which we call R_0 , for which halo dark matter will be captured due to self interactions with Earth bound dark matter.

When a dark matter particle, A' , from the halo passes through the dark matter accumulated in the Earth it will lose energy. The rate of energy loss is given by:

$$\frac{dE'}{dx} = -n_{A'}(x) \int_{E_R^{min}}^{E_R^{max}} \frac{d\sigma}{dE_R} E_R dE_R, \quad (9)$$

where x is the path of the dark matter particle. If the density of Earth bound dark matter particles is great enough, the dark matter particle A' will lose nearly all of its energy from self-interactions and become trapped within the Earth. The relevant cross-section for Rutherford scattering of a mirror nuclei with incoming velocity v on the mirror nuclei trapped within the Earth (here both assumed to have atomic number Z') and neglecting the form factors⁴ is given by

$$\frac{d\sigma}{dE_R} = \frac{\lambda}{E_R^2 v^2} \quad (10)$$

where

$$\lambda \equiv \frac{2\pi Z'^4 \alpha^2}{m_{A'}}. \quad (11)$$

With this cross-section, Eq.(9) indicates that dark matter particles will become trapped within the Earth if their trajectories are such that:

$$\begin{aligned} \int n_{A'}(x) dx &\gtrsim \frac{E_{in}'^2}{m_{A'} \lambda \log\left(\frac{E_R^{max}}{E_R^{min}}\right)} \\ &\gtrsim \left(\frac{10}{Z'}\right)^2 10^{16} \text{ cm}^{-2}, \end{aligned} \quad (12)$$

where $E_{in}' \sim \frac{1}{2} m_{A'} v_{rot}^2$ is the initial energy of the dark matter particle. The quantity $E_R^{max} = E_{in}'$ is the maximum kinematically allowed E_R , while $E_R^{min} \sim 1/(2r_b^2 m_{A'})$ (r_b is the Bohr radius) is set by the scale at which atomic screening becomes important.

⁴We employ natural units where $\hbar = c = 1$.

Approximating the trajectories of dark matter particles by straight lines, and defining the co-ordinate q as the distance along the trajectory with r_0 equal to the distance of closest approach to the Earth's center, we have:

$$\int n_{A'}(x)dx = \int n_{A'}(r = \sqrt{r_0^2 + q^2})dq . \quad (13)$$

Eq.(12,13) can be numerically solved for r_0 assuming a given $m_{A'}$ value. We find numerically that dark matter particles will get captured by self interactions provided their trajectories satisfy $r_0 \lesssim R_0$, with $R_0 \approx 4,000 \pm 700$ km, for $m_{A'}/m_p = 22 \pm 8^5$. Uncertainties in the ρ, T profile of the Earth give an (additional) estimated systematic uncertainty of order 5 – 10% in the determination of R_0 for a given $m_{A'}$ value. Thus, R_0 could in principle be as large as $\approx 5,500$ km. This completes our estimation of the ‘shielding radius’ R_0 .

4 Diurnal modulation effect due to shielding of the halo dark matter wind

We are now ready to estimate the effect of the shielding of the halo mirror dark matter due to its interactions with mirror dark matter trapped within the Earth. In principle halo dark matter interactions with ordinary matter can also shield or at least reduce the energy of halo dark matter particles[14]. However, for the case of mirror dark matter the latter effect is expected to be relatively small[23] especially if the kinetic mixing parameter ϵ satisfies the cosmology bound[28] $\epsilon \lesssim 10^{-9}$.

The direction of the Earth's motion through the halo, subtends an (average) angle $\approx 43^\circ$ with respect to the Earth's spin axis. There is a small annual modulation in this angle due to the Earth's rotation around the sun, which can be important and will be considered in the following section. Another relevant angle is the angle between the direction of the Earth's motion through the halo and the normal vector to the Earth's surface at the detector's location. This angle is denoted by ψ [Note that in ref.[14] this angle was denoted as θ]. The angle ψ , depends on the detector location and also the time of day, t :

$$\cos \psi = \cos \theta_{latitude} \sin \omega t \sin 43^\circ \pm \sin \theta_{latitude} \cos 43^\circ \quad (14)$$

where $\omega = 2\pi/T_d$ with $T_d = 1$ sidereal day (23.934 hours). In the above equation, the + [–] sign is relevant for a northern [southern] hemisphere detector, where $\theta_{latitude}$ is the north [south] latitude.

⁵Note that even if heavy $\sim \text{Fe}'$ component is responsible for the DAMA, CoGeNT and CRESST-II signals[4], it is reasonable to expect lighter components do dominate the shielding within the Earth.

Dark matter particles arriving at a detector originate predominately from a cone with axis in the direction of the Earth's motion through the halo and with the detector at its apex. The particles within the cone which pass through a distance from the Earth's center of $r_0 \lesssim R_0$ ($R_0 \approx 4,000$ km) will be shielded from the detector, while particles with $r_0 \gtrsim R_0$ will arrive unhindered by self-interactions. Because the direction of the cone of dark matter particles periodically changes due to the Earth's rotation, the proportion of dark matter particles shielded also modulates. Our task now is to estimate this effect for detectors in various locations.

The differential interaction rate is given by:

$$\begin{aligned} \frac{dR}{dE_R} &= N_T n_{A'} \int \frac{d\sigma}{dE_R} \frac{f_{A'}(\mathbf{v}, \mathbf{v}_E)}{k} |\mathbf{v}| d^3v \\ &= N_T n_{A'} \frac{\lambda}{E_R^2} \int_{|\mathbf{v}| > v_{min}(E_R)}^{\infty} \frac{f_{A'}(\mathbf{v}, \mathbf{v}_E)}{k|\mathbf{v}|} d^3v \end{aligned} \quad (15)$$

where N_T is the number of target atoms per kg of detector, $k = (\pi v_0^2 [A'])^{3/2}$ is the Maxwellian distribution normalization factor and $n_{A'} = \rho_{dm} \xi_{A'}/m_{A'}$ is the number density of the halo mirror nuclei A' at the Earth's location (we take $\rho_{dm} = 0.3$ GeV/cm³). [This should not be confused with the number density of trapped mirror nuclei in the Earth, despite the similarity in the notation!]. Here \mathbf{v} is the velocity of the halo particles relative to the Earth and \mathbf{v}_E is the velocity of the Earth relative to the galactic halo. The halo distribution function in the reference frame of the Earth is given by, $f_{A'}(\mathbf{v}, \mathbf{v}_E)/k = (\pi v_0^2 [A'])^{-3/2} \exp(-(\mathbf{v} + \mathbf{v}_E)^2/v_0^2 [A'])$. Note that the lower velocity limit, $v_{min}(E_R)$, is given by the kinematic relation:

$$v_{min} = \sqrt{\frac{(m_A + m_{A'})^2 E_R}{2m_A m_{A'}}}. \quad (16)$$

The interaction rate depends on the velocity integral in Eq.(15),

$$I \equiv \int_{|\mathbf{v}| > v_{min}(E_R)}^{\infty} \frac{f_{A'}(\mathbf{v}, \mathbf{v}_E)}{k|\mathbf{v}|} d^3v. \quad (17)$$

This integral can be modified to incorporate the effect of shielding of the halo dark matter by the Earth bound mirror matter, by multiplying the integrand by the quantity $g(\theta, \phi, \psi)$, where

$$\begin{aligned} g(\theta, \phi, \psi) &= 0 \text{ if } d_{min} < R_0 \\ &= 1 \text{ if } d_{min} > R_0. \end{aligned} \quad (18)$$

Here d_{min} is the distance of closest approach to the center of the Earth experienced by the particle trajectories. We show in the appendix that d_{min} is given by:

$$\begin{aligned} d_{min}^2(\theta, \phi, \psi) &= R_E^2 [1 - f^2(\theta, \phi, \psi)] \text{ if } f(\theta, \phi, \psi) > 0 \\ &= R_E^2 \text{ if } f(\theta, \phi, \psi) < 0 \end{aligned} \quad (19)$$

where

$$f(\theta, \phi, \psi) = \sin \theta \sin \psi \sin \phi - \cos \theta \cos \psi \quad (20)$$

and $R_E \simeq 6378$ km is the radius of the Earth. Thus, the shielding effects can be incorporated by replacing I , defined in Eq.(17), with:

$$\begin{aligned} I[\psi(t)] &\equiv \int_{|\mathbf{v}| > v_{min}(E_R)}^{\infty} \frac{f_{A'}(\mathbf{v}, \mathbf{v}_E)}{k|\mathbf{v}|} g(\theta, \phi, \psi) d^3v \\ &\equiv \int_{-1}^1 \int_0^{2\pi} \int_{|\mathbf{v}| > v_{min}(E_R)}^{\infty} \frac{f_{A'}(\mathbf{v}, \mathbf{v}_E)}{k} g(\theta, \phi, \psi) |\mathbf{v}| d|\mathbf{v}| d\phi d \cos \theta . \end{aligned} \quad (21)$$

We are now in a position to evaluate the effect of shielding of mirror dark matter expected for experiments at various locations. We compute the quantity

$$\mathcal{R} \equiv 100 \times \left(1 - \frac{I[\psi(t)]}{I} \right) \quad (22)$$

which gives the percentage rate reduction in the interaction rate due to shielding of dark matter in the core of the Earth. In figure 3a we give results for \mathcal{R} , with $E_R = 6.7$ keV_{NR} for Na target, relevant for the DAMA set up at Gran Sasso with north latitude = 42.5°. We consider two reference sets of parameters, the first one assumes the ‘standard’ parameters $R_0 = 4,000$ km and $\bar{m} = 1.1$ GeV. The second possibility assumes ‘optimistic’ values $R_0 = 5,500$ km and $\bar{m} = 3.0$ GeV. Figure 3a shows that even with the optimistic parameters, the diurnal signal modulation is expected to be relatively small for DAMA/Libra at Gran Sasso. Thus the lack of a diurnal modulation in the DAMA/NaI experiment[29] does not significantly constrain any parameter space. Currently DAMA/Libra is running with a lower energy threshold which will make them more sensitive to the diurnal effect simply because the signal rate is much higher at lower energies, $dR/dE_R \propto 1/E_R^2$. Thus, for optimistic parameters DAMA/Libra might possibly detect a small diurnal modulation.

The CoGeNT Ge detector has been operating in the Soudan underground laboratory, which has north latitude of 48°. This is a little further north than that of Gran Sasso, so the diurnal modulation effect expected at Soudan is smaller than that for DAMA/Libra. However, for the CDEX/Texono Ge detectors[30] located at Jin-Ping underground laboratory at north latitude 28°, the effects are expected to be larger. In figure 3b we give the results for these detectors at $E_R = 2$ keV_{NR}.

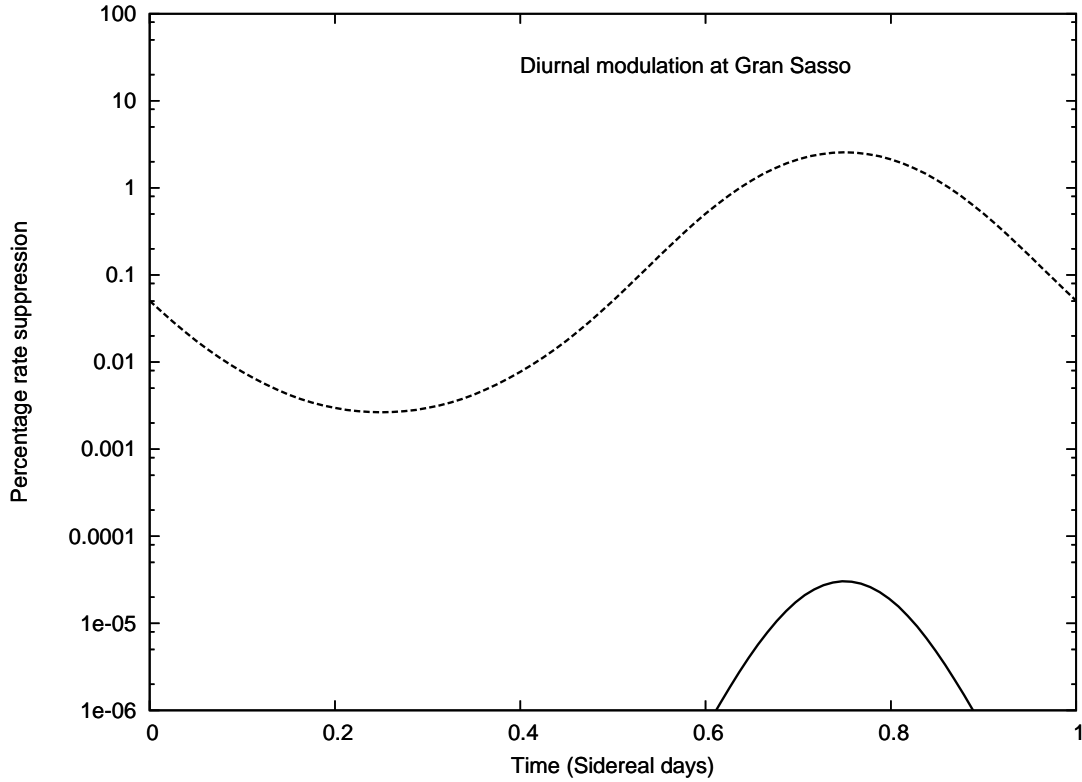


Figure 3a: Percentage rate suppression due to the shielding of dark matter in the Earth’s core versus time, for a Na detector at Gran Sasso. A reference energy of 6.7 keV_{NR} has been assumed. Both the captured and interacting dark matter particles are assumed to have the mass $m_{A'} = 22m_p$. The solid line assumes ‘standard’ parameters where the shielding radius is taken to be $R_0 = 4,000 \text{ km}$ and the halo velocity dispersion is given in Eq.(3) assuming $\bar{m} = 1.1 \text{ GeV}$. The dashed line is for the more optimistic case considered where $R_0 = 5,500 \text{ km}$ and $\bar{m} = 3.0 \text{ GeV}$.

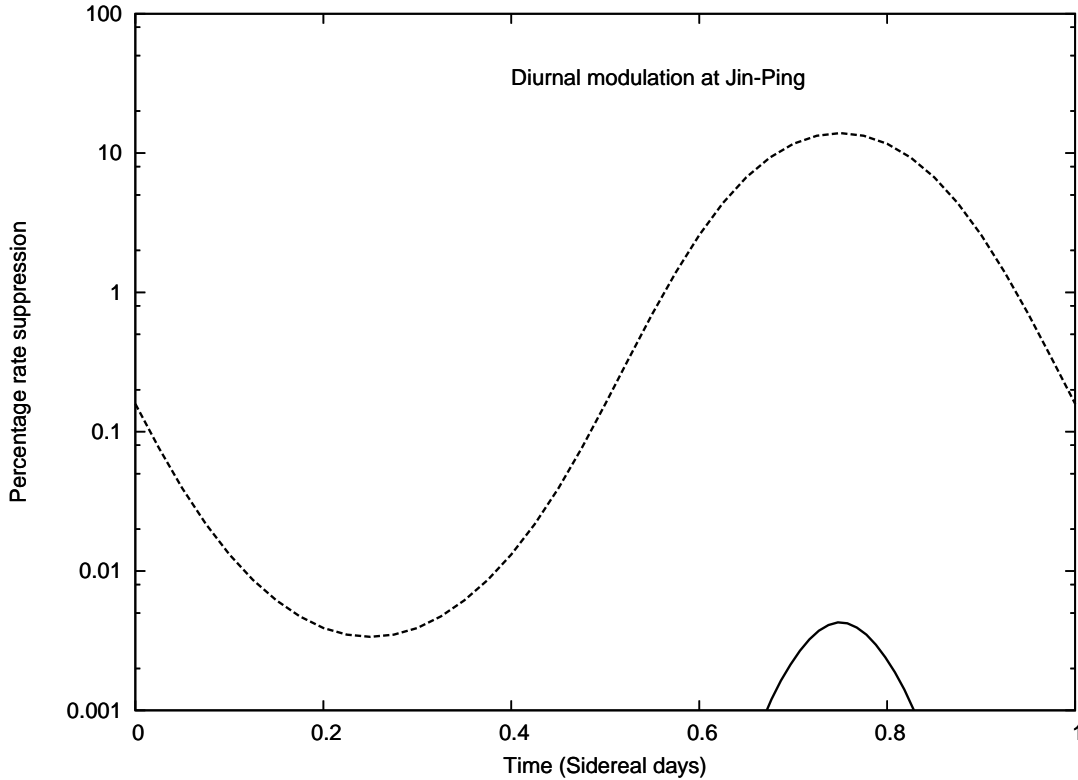


Figure 3b: Same as figure 3a except that the Na detector at Gran Sasso is changed to CDEX/Texono Ge detector at Jin-Ping underground laboratory (a reference energy of 2 keV_{NR} is assumed).

The effects in existing detectors in the northern hemisphere are not very large, although there is some possibility of observing the effect with optimistic parameters, especially at the Jin-Ping laboratory. Of course, the reason that the shielding effect is not so large is simply because all of the existing detectors are located in the northern hemisphere. The effect becomes dramatically bigger for a detector located in the southern hemisphere because the halo dark matter particles then have a much larger probability of passing through the center of the Earth. We illustrate this in figure 3c which gives results for the CoGeNT detector relocated to the Sierra Grande laboratory in Argentina, with south latitude 41.6° . As the figure shows, the variation ranges from near zero to 100 %. At Soudan, the CoGeNT spectrum is consistent with around 3 dark matter signal events per day per 0.3 kg . We estimate then that the diurnal effect at Sierra Grande would be so large that just 30 days of data would be sufficient to yield a 5σ discovery of dark matter with CoGeNT's $\sim 0.3 \text{ kg}$ detector.

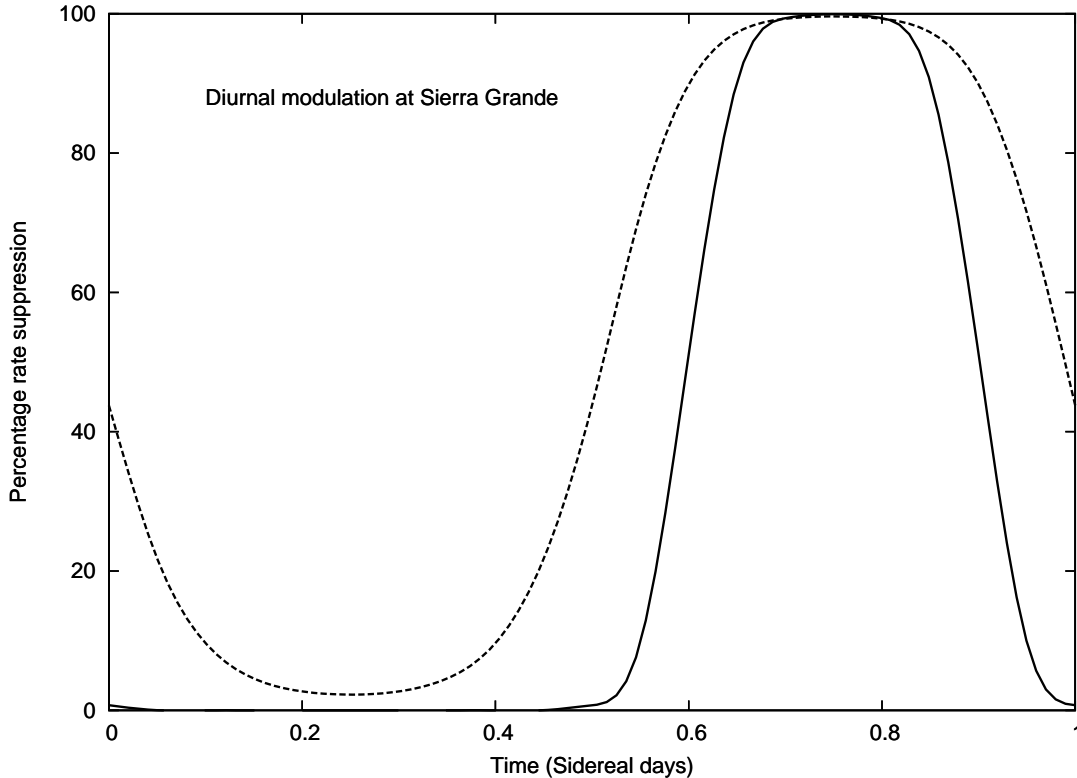


Figure 3c: Same as figure 3a except that the Na detector at Gran Sasso is changed to CoGeNT Ge detector relocated to Sierra Grande, Argentina.

Finally, we comment on the proposal to place a NaI detector at the South Pole[31]. Interestingly, the South Pole is the only point in the southern hemisphere where the diurnal modulation effect is absent. For a detector at the south pole we find a constant 32% [85%] rate suppression for the standard [optimistic] parameter values.

5 Annual variation of the diurnal modulation

The proportion of the Earth which shields dark matter particles has both a diurnal variation and an annual variation. The annual variation, which we have hitherto neglected, arises because of the variation of the direction of the Earth's motion through the halo, due to the Earth's motion around the sun. In this section we examine this effect.

The direction of the Earth's motion through the halo, subtends an angle $\theta_1(t)$ with respect to the Earth's spin axis. On average this angle is approximately 43° , but varies during the year. To evaluate this angle at a given time, t , define a right-angled co-ordinate system with the z -axis in the direction of the normal to the ecliptic plane, x -axis in the direction of the sun relative to the Earth and y -axis in the direction of the Earth's motion around the sun. In this co-ordinate system, for an observer at rest with respect to the halo, the Earth's velocity vector is

$$\begin{aligned}\mathbf{v}_E &= v_\odot \left[-\sin 30^\circ \cos 2\pi \frac{(t-t_1)}{T}, -\sin 30^\circ \sin 2\pi \frac{(t-t_1)}{T}, \cos 30^\circ \right] + v_\oplus [0, 1, 0] \\ &= v_\odot \left[-\sin 30^\circ \cos 2\pi \frac{(t-t_1)}{T}, -\sin 30^\circ \sin 2\pi \frac{(t-t_1)}{T} + y, \cos 30^\circ \right] \quad (23)\end{aligned}$$

where $t_1 = 152.5 \text{ days} + 0.25 \text{ years} \simeq 244 \text{ days}$, $T = 1 \text{ year}$ and $y = v_\oplus/v_\odot \approx 30/240 \approx 0.125$. The angle, 30° is the angle between the normal of the ecliptic plane and the sun's direction of motion through the halo. The Earth's spin axis has the direction:

$$\mathbf{L}_{spin} = \left[\sin 23.5^\circ \cos 2\pi \frac{(t-t_2)}{T}, \sin 23.5^\circ \sin 2\pi \frac{(t-t_2)}{T}, \cos 23.5^\circ \right] \quad (24)$$

where $t_2 \simeq 172 \text{ days}$ (northern summer solstice). The angle 23.5° is the tilt of the Earth's spin axis relative to the normal of the ecliptic plane. The angle $\theta_1(t)$, is then given by

$$\begin{aligned}\cos \theta_1 &= \frac{\mathbf{v}_E \cdot \mathbf{L}_{spin}}{|\mathbf{v}_E| |\mathbf{L}_{spin}|} \\ &\simeq \cos \bar{\theta}_1 + y \left[\cos \bar{\theta}_1 \sin 30^\circ \sin 2\pi \frac{(t-t_1)}{T} + \sin 23.5^\circ \sin 2\pi \frac{(t-t_2)}{T} \right] \quad (25)\end{aligned}$$

where

$$\cos \bar{\theta}_1 = \cos 30^\circ \cos 23.5^\circ - \sin 30^\circ \sin 23.5^\circ \cos 2\pi \frac{(t_1-t_2)}{T} \quad (26)$$

Thus, we see that the angle $\theta_1(t)$ is not actually a constant, but has a small variation due to the earth's motion around the sun ($y \neq 0$).

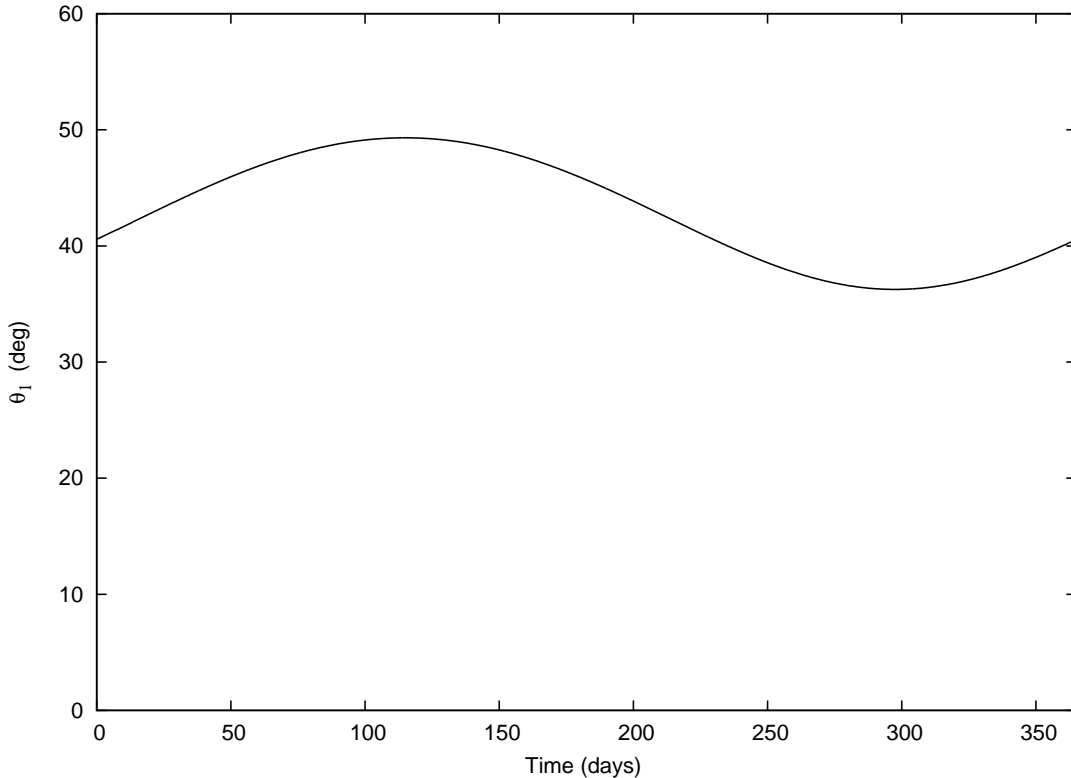


Figure 4: The angle, $\theta_1(t)$ versus time. [This is the angle between the Earth’s spin axis and the Earth’s direction of motion through the halo].

In figure 4, we plot $\theta_1(t)$ over its period of one year (where $t = 0$ corresponds to January 1). As the figure shows, we find that θ_1 has a maximum of 49.3° (April 25) and minimum of 36.3° (October 25). This variation is relatively unimportant for a detector in the southern hemisphere⁶. For a detector in the northern hemisphere we expect the largest diurnal signal to occur when θ_1 is a maximum and thus we anticipate that the largest diurnal signal will occur in April. The effect of the θ_1 variation can be estimated by repeating the analysis of the previous section, with 43° in Eq.(14) replaced with 49.3 and 36.3 [in general 43° is replaced by $\theta_1(t)$ in Eq.(14)]. In figure 5a we plot the percentage rate suppression for the optimistic parameter choice for a detector located at Gran Sasso. The figure shows that the variation of the diurnal signal during the year is significant. Figure 5b is the corresponding results for a detector located at Jin-Ping Underground laboratory. Clearly the March

⁶For the special case of a detector at the South Pole, there is no diurnal signal as noted earlier, but there is a rate suppression which annually modulates slightly due to the variation of $\theta_1(t)$.

- May quarter provides the best window to detect the diurnal signal for a northern hemisphere detector. The CDEX experiment in Jin-Ping, currently running with a 1 kg Ge PC detector, with plans to upgrade to > 10 kg has an excellent opportunity to observe the diurnal signal. The 250 kg DAMA/Libra detector, currently running with lower threshold, also has a very good chance to see such a signal in the March-May quarter.

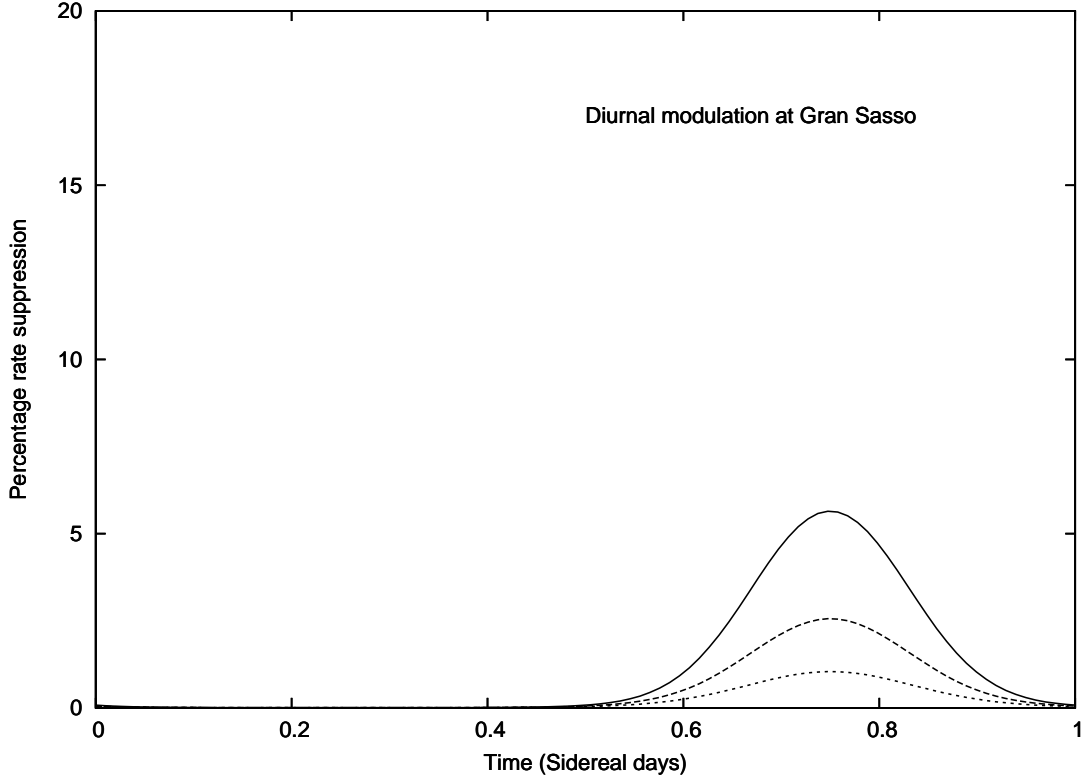


Figure 5a: Percentage rate suppression due to the shielding of dark matter in the Earth’s core versus time, for a Na detector at Gran Sasso. A reference energy of 6.7 keV_{NR} has been assumed. Both the captured and interacting dark matter particles are taken to have the reference mass $m_{A'} = 22m_p$. We have assumed the optimistic case with shielding radius of $R_0 = 5,500 \text{ km}$ and the halo velocity dispersion is given in Eq.(3) with $\bar{m} = 3.0 \text{ GeV}$. The solid line assumes $\theta_1 = 49.3^\circ$ (April 25), the dashed line assumes $\theta_1 = 43^\circ$, (Yearly average) and the dotted line assumes $\theta_1 = 36.3^\circ$ (October 25).

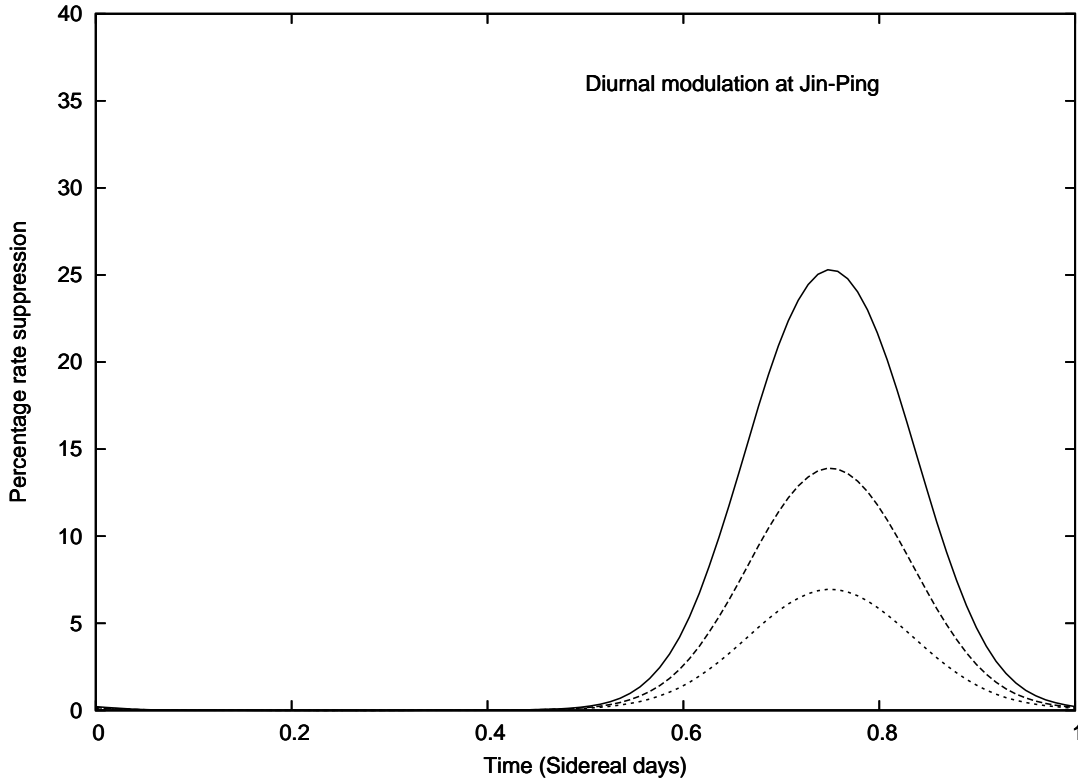


Figure 5b: Same as figure 5a except that the Na detector at Gran Sasso is changed to CDEX/TeXono Ge detector at Jin-Ping underground laboratory (a reference energy of 2 keV_{NR} is assumed).

6 Conclusion

Mirror and more generic hidden sector dark matter models can simultaneously explain the DAMA, CoGeNT and CRESST-II dark matter signals consistently with the null results of the other experiments. This type of dark matter can be captured by the Earth and shield detectors because it is self-interacting. This effect will lead to a diurnal modulation in dark matter detectors. We have estimated the size of this effect for dark matter detectors in various locations.

Current dark matter detectors in the northern hemisphere are not so sensitive to the diurnal modulation although there is an exciting possibility that it can be detected at Jin-Ping and even in DAMA/Libra for optimistic parameter choices. We have also found that the diurnal signal for detectors located in the northern hemisphere varies during the year, peaking in April.

The situation changes dramatically for detectors located in the southern hemisphere where the dark matter wind passes directly through the core of the Earth for part of the day. In particular, if the CoGeNT detector were moved to e.g. Sierra Grande, Argentina then a 5σ dark matter discovery would be possible in around 30 days of operation.

Appendix: Calculation of d_{min}

In this appendix we derive Eq.(19). Recall dark matter particles reaching a detector originate predominately from a cone centered along the Earth's direction of motion through the halo. Recall also that ψ is the angle between the normal vector to the Earth's surface at the detector's location and the axis of this cone. We assume that particles form straight line trajectories. Let us introduce a co-ordinate system with the detector at the origin. We use polar co-ordinates with the z - *axis* aligned with the direction of the Earth's motion through the halo. The points along the particle trajectory are given by $(r \sin \theta \sin \phi, r \sin \theta \cos \phi, r \cos \theta)$. In this co-ordinate system (suitably rotated in the azimuthal direction) the location of Earth's center is $(R_E \sin \psi, 0, -R_E \cos \psi)$, where $R_E \simeq 6378$ km is the Earth's radius. The distance between the Earth's center and a point along the particle trajectory is then given by

$$d^2 = R_E^2 + r^2 + 2R_E r (\cos \theta \cos \psi - \sin \theta \sin \psi \sin \phi) . \quad (27)$$

We need to determine d_{min} which is the distance of closest approach to the Earth's center as we vary r keeping θ , ϕ and ψ fixed. The value of r where this occurs can be determined by minimizing d^2 with respect to r , i.e. from $\partial d^2 / \partial r = 0$. Evaluating this value of r and substituting it back into Eq.(27) we obtain Eq.(19) as the solution. This completes the outline of the derivation of Eq.(19).

Acknowledgments

This work was supported by the Australian Research Council.

References

- [1] R. Foot, H. Lew and R. R. Volkas, Phys. Lett. B272, 67 (1991); Mod. Phys. Lett. A7, 2567 (1992).
- [2] R. Foot, Phys. Lett. B703, 7 (2011) [arXiv: 1106.2688]; Phys. Lett. B692: 65 (2010) [arXiv: 1004.1424].

- [3] R. Foot, Phys. Rev. D82: 095001 (2010) [arXiv: 1008.0685].
- [4] R. Foot, arXiv: 1203.2387.
- [5] R. Bernabei *et al.* (DAMA Collaboration), Riv. Nuovo Cimento. 26, 1 (2003) [astro-ph/0307403]; Int. J. Mod. Phys. D13, 2127 (2004); Phys. Lett. B480, 23 (2000); Eur. Phys. J. C56: 333 (2008) [arXiv:0804.2741]; Eur. Phys. J. C67, 39 (2010) [arXiv: 1002.1028].
- [6] C. E. Aalseth *et al.* (CoGeNT Collaboration), Phys. Rev. Lett. 106: 131301 (2011) [arXiv:1002.4703]; Phys.Rev.Lett. 107 (2011) 141301 [arXiv: 1106.0650].
- [7] G. Angloher *et al.*, (CRESST Collaboration), arXiv:1109.0702.
- [8] Z. Ahmed *et al* (CDMS Collaboration), Science 327: 1619 (2010) [arXiv: 0912.3592].
- [9] E. Aprile *et al.* (XENON100 Collaboration), Phys. Rev. Lett. 107, 131302 (2011) [arXiv:1104.2549].
- [10] J. Angle *et al.* [XENON10 Collaboration], Phys. Rev. Lett. 107, 051301 (2011) [arXiv:1104.3088].
- [11] Z. Ahmed *et al.* [CDMS-II Collaboration], Phys. Rev. Lett. 106, 131302 (2011) [arXiv:1011.2482].
- [12] J. I. Collar, arXiv:1103.3481 ; arXiv:1106.0653 .
- [13] See e.g. D. N. Spergel and P. J. Steinhardt, Phys. Rev. Lett. 84, 3760 (2000) [astro-ph/9909386]; A. E. Faraggi and M. Pospelov, Astropart. Phys. 16, 451 (2002) [arXiv: hep-ph/0008223]; S. Mitra, Phys. Rev. D71 121302 (2005) [astro-ph/0409121]; J. L. Feng, H. Tu and H-B. Yu, JCAP 0810: 43 (2008) [arXiv: 0808.2318]; H. An, S-L. Chen, R. N. Mohapatra, S. Nussinov and Y. Zhang, Phys. Rev. D82, 023533 (2010) [arXiv: 1004.3296]; N. Fornengo, P. Panci and M. Regis, arXiv: 1108.4661; J-W. Cui, H-J. He, L-C. Lv and F-R. Yin, arXiv: 1110.6893.
- [14] J. I. Collar and F. T. Avignone III, Phys. Lett. B275, 181 (1992); Phys.Rev. D47 5238 (1993); F. Hasenbalg *et al.*, Phys.Rev. D55, 7350 (1997).
- [15] D. E. Di Gregorio *et al.*, Nucl.Phys.Proc.Suppl. 48, 56 (1996).
- [16] R. Foot, Phys. Rev. D78, 043529 (2008) [arXiv: 0804.4518].

- [17] R. Foot and X-G. He, Phys. Lett. B267, 509 (1991).
- [18] B. Holdom, Phys. Lett. B166, 196 (1986).
- [19] R. Foot, Phys. Lett. B699, 230 (2011) [arXiv:1011.5078].
- [20] R. Foot, Int. J. Mod. Phys. D13, 2161 (2004) [astro-ph/0407623]; P. Ciarcelluti, Int. J. Mod. Phys. D19: 2151 (2010) [arXiv: 1102.5530].
- [21] H. M. Hodges, Phys. Rev. D47, 456 (1993); Z. Berezhiani, D. Comelli and F. L. Villante, Phys. Lett. B503, 362 (2001) [hep-ph/0008105]; L. Bento and Z. Berezhiani, Phys. Rev. Lett. 87, 231304 (2001) [hep-ph/0107281]; A. Yu. Ignatiev and R. R. Volkas, Phys. Rev. D68, 023518 (2003) [hep-ph/0304260]; R. Foot and R. R. Volkas, Phys. Rev. D68, 021304 (2003) [hep-ph/0304261]; Phys. Rev. D69, 123510 (2004) [hep-ph/0402267]; Z. Berezhiani, P. Ciarcelluti, D. Comelli and F. L. Villante, Int. J. Mod. Phys. D14, 107 (2005) [astro-ph/0312605]; P. Ciarcelluti, Int. J. Mod. Phys. D14, 187 (2005) [astro-ph/0409630]; Int. J. Mod. Phys. D14, 223 (2005) [astro-ph/0409633]. For pioneering work, see: S. I. Blinnikov and M. Yu. Khlopov, Sov. J. Nucl. Phys. 36, 472 (1981); Sov. Astron. 27, 371 (1983).
- [22] R. Foot and R. R. Volkas, Phys. Rev. D70, 123508 (2004) [astro-ph/0407522].
- [23] R. Foot, Phys. Rev. D69, 036001 (2004) [hep-ph/0308254].
- [24] R. Foot, Mod. Phys. Lett. A19, 1841 (2004) [astro-ph/0405362]; Phys. Rev. D74, 023514 (2006) [astro-ph/0510705].
- [25] P. Ciarcelluti and R. Foot, Phys. Lett. B690, 462 (2010) [arXiv:1003.0880].
- [26] A. Y. Ignatiev and R. R. Volkas, Phys. Rev. D62, 023508 (2000) [arXiv:hep-ph/0005125].
- [27] A. M. Dziewonski and D. L. Anderson, Phys. Earth Planet. Interiors 25, 297 (1981).
- [28] P. Ciarcelluti and R. Foot, Phys. Lett. B679, 278 (2009) [arXiv: 0809.4438].
- [29] R. Bernabei *et al.*, (DAMA Collaboration), Nuovo Cim. A112, 1541 (1999).
- [30] H. Wong, On behalf of the CDEX-Texono Collaboration, Talk at TAUP, Munich, September 2011.
- [31] R. Maruyama, on behalf of DM-ice collaboration, talk at TAUP, Sept. 2011.